

Residues Important for Nitrate/Proton Coupling in Plant and Mammalian CLC Transporters*

Received for publication, February 19, 2009, and in revised form, March 3, 2009. Published, JBC Papers in Press, March 4, 2009, DOI 10.1074/jbc.M901170200

Eun-Yeong Bergsdorf[‡], Anselm A. Zdebik^{‡§}, and Thomas J. Jentsch^{‡1}

From the [‡]Department of Physiology and Pathology of Ion Transport, Leibniz-Institut für Molekulare Pharmakologie (FMP) and Max-Delbrück-Centrum für Molekulare Medizin (MDC), D-13125 Berlin, Germany and the [§]Department of Neuroscience, Physiology and Pharmacology, London Epithelial Group, Royal Free Campus, University College London (UCL), London NW3 2PF, United Kingdom

Members of the CLC gene family either function as chloride channels or as anion/proton exchangers. The plant AtCLC-a uses the pH gradient across the vacuolar membrane to accumulate the nutrient NO₃⁻ in this organelle. When AtCLC-a was expressed in *Xenopus* oocytes, it mediated NO₃⁻/H⁺ exchange and less efficiently mediated Cl⁻/H⁺ exchange. Mutating the “gating glutamate” Glu-203 to alanine resulted in an uncoupled anion conductance that was larger for Cl⁻ than NO₃⁻. Replacing the “proton glutamate” Glu-270 by alanine abolished currents. These could be restored by the uncoupling E203A mutation. Whereas mammalian endosomal CIC-4 and CIC-5 mediate stoichiometrically coupled 2Cl⁻/H⁺ exchange, their NO₃⁻ transport is largely uncoupled from protons. By contrast, the AtCLC-a-mediated NO₃⁻ accumulation in plant vacuoles requires tight NO₃⁻/H⁺ coupling. Comparison of AtCLC-a and CIC-5 sequences identified a proline in AtCLC-a that is replaced by serine in all mammalian CLC isoforms. When this proline was mutated to serine (P160S), Cl⁻/H⁺ exchange of AtCLC-a proceeded as efficiently as NO₃⁻/H⁺ exchange, suggesting a role of this residue in NO₃⁻/H⁺ exchange. Indeed, when the corresponding serine of CIC-5 was replaced by proline, this Cl⁻/H⁺ exchanger gained efficient NO₃⁻/H⁺ coupling. When inserted into the model *Torpedo* chloride channel CIC-0, the equivalent mutation increased nitrate relative to chloride conductance. Hence, proline in the CLC pore signature sequence is important for NO₃⁻/H⁺ exchange and NO₃⁻ conductance both in plants and mammals. Gating and proton glutamates play similar roles in bacterial, plant, and mammalian CLC anion/proton exchangers.

CLC proteins are found in all phyla from bacteria to humans and either mediate electrogenic anion/proton exchange or function as chloride channels (1). In mammals, the roles of plasma membrane CLC Cl⁻ channels include transepithelial transport (2–5) and control of muscle excitability (6), whereas vesicular CLC exchangers may facilitate endocytosis (7) and lysosomal function (8–10) by electrically shunting vesicular proton pump currents (11). In the plant *Arabidopsis thaliana*,

there are seven CLC isoforms (AtCLC-a–AtCLC-g)² (12–15), which may mostly reside in intracellular membranes. AtCLC-a uses the pH gradient across the vacuolar membrane to transport the nutrient nitrate into that organelle (16). This secondary active transport requires a tightly coupled NO₃⁻/H⁺ exchange. Astonishingly, however, mammalian CIC-4 and -5 and bacterial EcCIC-1 (one of the two CLC isoforms in *Escherichia coli*) display tightly coupled Cl⁻/H⁺ exchange, but anion flux is largely uncoupled from H⁺ when NO₃⁻ is transported (17–21). The lack of appropriate expression systems for plant CLC transporters (12) has so far impeded structure-function analysis that may shed light on the ability of AtCLC-a to perform efficient NO₃⁻/H⁺ exchange. This dearth of data contrasts with the extensive mutagenesis work performed with CLC proteins from animals and bacteria.

The crystal structure of bacterial CLC homologues (22, 23) and the investigation of mutants (17, 19–21, 24–29) have yielded important insights into their structure and function. CLC proteins form dimers with two largely independent permeation pathways (22, 25, 30, 31). Each of the monomers displays two anion binding sites (22). A third binding site is observed when a certain key glutamate residue, which is located halfway in the permeation pathway of almost all CLC proteins, is mutated to alanine (23). Mutating this gating glutamate in CLC Cl⁻ channels strongly affects or even completely suppresses single pore gating (23), whereas CLC exchangers are transformed by such mutations into pure anion conductances that are not coupled to proton transport (17, 19, 20). Another key glutamate, located at the cytoplasmic surface of the CLC monomer, seems to be a hallmark of CLC anion/proton exchangers. Mutating this proton glutamate to nontitratable amino acids uncouples anion transport from protons in the bacterial EcCIC-1 protein (27) but seems to abolish transport altogether in mammalian CIC-4 and -5 (21). In those latter proteins, anion transport could be restored by additionally introducing an uncoupling mutation at the gating glutamate (21).

The functional complementation by AtCLC-c and -d (12, 32) of growth phenotypes of a yeast strain deleted for the single

* This work was supported by a Deutsche Forschungsgemeinschaft grant (to A. A. Z. and T. J. J.) and by the Leibniz Graduate School of Biophysics.

¹ To whom correspondence should be addressed: FMP/MDC, Robert-Rössle-Str. 10, D-13125 Berlin, Germany. Fax: 49-30-9406-2960; E-mail: Jentsch@fmp-berlin.de.

² The abbreviations used are: AtCLC-*n*, member *n* of the CLC family of Cl⁻ channels and transporters in the plant *Arabidopsis thaliana*; CIC-*n*, member *n* of the CLC family of chloride channel and transporters (in animals); pH_i, intracellular pH; pH_o, extracellular pH; I(NO₃⁻) and I(Cl⁻), current in the presence of NO₃⁻ and Cl⁻, respectively, which in CLC exchangers also involves an H⁺ component; WT, wild-type; MES, 2-(*N*-morpholino)ethanesulfonic acid; BCECF, 2',7'-bis(2-carboxyethyl)-5(6)-carboxyfluorescein.

yeast CLC Gef1 (33) suggested that these plant CLC proteins function in anion transport but could not reveal details of their biophysical properties. We report here the first functional expression of a plant CLC in animal cells. Expression of wild-type (WT) and mutant AtCLC-a in *Xenopus* oocytes indicate a general role of gating and proton glutamate residues in anion/proton coupling across different isoforms and species. We identified a proline in the CLC signature sequence of AtCLC-a that plays a crucial role in NO_3^-/H^+ exchange. Mutating it to serine, the residue present in mammalian CLC proteins at this position, rendered AtCLC-a Cl^-/H^+ exchange as efficient as NO_3^-/H^+ exchange. Conversely, changing the corresponding serine of CLC-5 to proline converted it into an efficient NO_3^-/H^+ exchanger. When proline replaced the critical serine in *Torpedo* CLC-0, the relative NO_3^- conductance of this model Cl^- channel was drastically increased, and "fast" protopore gating was slowed.

EXPERIMENTAL PROCEDURES

Molecular Biology—cDNAs of *A. thaliana* AtCLC-a (12), rat CLC-5 (34), and *Torpedo marmorata* CLC-0 (35) were cloned into the pTLN (36) expression vector. Mutations were generated by recombinant PCR and confirmed by sequencing. Capped cRNA was transcribed from linearized plasmids using the Ambion mMESSAGE mMACHINE kit (SP6 RNA polymerase for pTLN) according to the manufacturer's instructions.

Expression in *Xenopus* Oocyte and Two-electrode Voltage-Clamp Studies—Pieces of ovary were obtained by surgery from deeply anesthetized (0.1% tricaine; Sigma) pigmented or albino *Xenopus laevis* frogs. Oocytes were prepared by manual dissection and collagenase A (Roche Applied Science) digestion. 23 ng (CLC-5), 46–50 ng (AtCLC-a), or 1–3 ng (CLC-0) of cRNA were injected into oocytes. Oocytes were kept in ND96 solution (containing 96 mM NaCl, 2 mM KCl, 1.8 mM CaCl_2 , 1 mM MgCl_2 , 5 mM HEPES, pH 7.5) at 17 °C for 1–2 days (CLC-0), 3–4 days (CLC-5), or for 5–6 days (AtCLC-a). Two-electrode voltage clamping was performed at room temperature (20–24 °C) using a TEC10 amplifier (npi Electronics, Tamm, Germany) and pClamp9 software (Molecular Devices). The standard bath solution contained 96 mM NaCl, 2 mM K^+ gluconate, 5 mM Ca^{2+} D-gluconate, 1.2 mM MgSO_4 , 5 mM HEPES, pH 7.5 (or MES for buffering to pH 5.5 or 6.5; Tris for pH 8.5). For some experiments, NaCl was substituted with equal amounts of either NaNO_3 , NaBr, or NaI. Ag/AgCl electrodes and 3 M KCl agar bridges were used as reference and bath electrodes, respectively.

Measurement of Relative Intracellular pH Changes Using the "Fluorocyte" Device—Proton transport was measured semiquantitatively by monitoring intracellular fluorescence signal changes using the Fluorocyte device (21). Briefly, 23 nl of saturated aqueous solution of the pH indicator BCECF (Molecular Probes) were injected into oocytes 10–30 min before measurements. Oocytes were placed over a hole 0.8 mm in diameter, through which BCECF fluorescence changes were measured in response to pulse trains, which served to reduce the possible activation of endogenous oocyte currents. Starting from a holding voltage of -60 mV, depolarizing pulse trains clamped oocytes to $+90$ mV for 400 ms and -60 mV for 100 ms, whereas

hyperpolarizing pulse trains started from -30 mV and clamped to -160 mV for 400 ms and to -30 mV for 100 ms. BCECF fluorescence was measured with a photodiode and digitally Bessel-filtered at 0.3 Hz. These nonratiometric measurements generally show drifts owed to bleaching or intracellular dye distribution (21) but allow for sensitive measurements of pH changes upon changes in voltage or external ion composition.

RESULTS

Previous attempts to functionally express plant CLC proteins in animal cells proved unsuccessful (12). However, when *Xenopus* oocytes were measured 5 or more days after injecting AtCLC-a cRNA, currents well above background levels were observed in two-electrode voltage-clamp experiments (Fig. 1). These outwardly rectifying currents were roughly 30% larger when extracellular chloride was replaced by nitrate (NO_3^-) (Fig. 1, A–C), smaller with extracellular iodide, and nearly unchanged with a replacement by bromide (Fig. 1C). Reversal potentials indicated that the apparent anion permeability was larger for NO_3^- than for the other anions tested. It should be noted that for CLC exchangers, the observed apparent permeabilities and conductances represent those of coupled anion/proton exchange rather than diffusive anion transport. Contrasting with the slow activation of currents by depolarization observed in plant vacuoles (16), heterologously expressed AtCLC-a currents almost totally lacked time-dependent relaxations (Fig. 1, A and B). Like currents elicited by CLC-4 or -5 (26), AtCLC-a currents were reduced by acidic extracellular pH (pH_o) (Fig. 1, D–F). With extracellular NO_3^- , the extracellular pH had to be more acidic to obtain the same degree of current decrease as with Cl^- (Fig. 1F).

We next explored proton transport of AtCLC-a by measuring semiquantitatively the pH_i of voltage-clamped oocytes using the Fluorocyte system (21). Net ion transport was elicited by strongly depolarizing oocytes to $+90$ mV. Because prolonged strong depolarization can elicit endogenous transport processes in oocytes, trains of depolarizing pulses were used instead (20, 21). An inside-positive voltage should lead to anion influx and proton efflux through electrogenic anion/proton exchangers. Pulsing AtCLC-a-expressing oocytes to positive voltages indeed induced intracellular alkalinization (Fig. 1G). Importantly, alkalinization was also observed when protons were extruded against their electrochemical potential (at pH_o 5.5), suggesting that their transport is driven by the coupled anion entry (Fig. 1H). Under either condition (pH_o 7.5 or 5.5), alkalinization occurred more rapidly with extracellular NO_3^- than with Cl^- . This shows that AtCLC-a more efficiently mediates NO_3^-/H^+ exchange than Cl^-/H^+ exchange, a finding compatible with its role in accumulating NO_3^- in plant vacuoles (16, 37). In contrast with CLC-4 and -5 (26), AtCLC-a mediates robust currents also at negative voltages (Fig. 1, A–E). Accordingly, and in contrast to CLC-5 (see Fig. 5H), AtCLC-a mediated proton influx when oocytes were pulsed to negative voltages (-160 mV) (Fig. 1I). Substituting extracellular Cl^- by NO_3^- failed to influence the rate of acidification because proton influx is coupled to an efflux of anions from the interior of oocytes.

In EcCLC-1 and CLC-4 and -5, a certain gating glutamate is important for coupling chloride fluxes to proton countertrans-

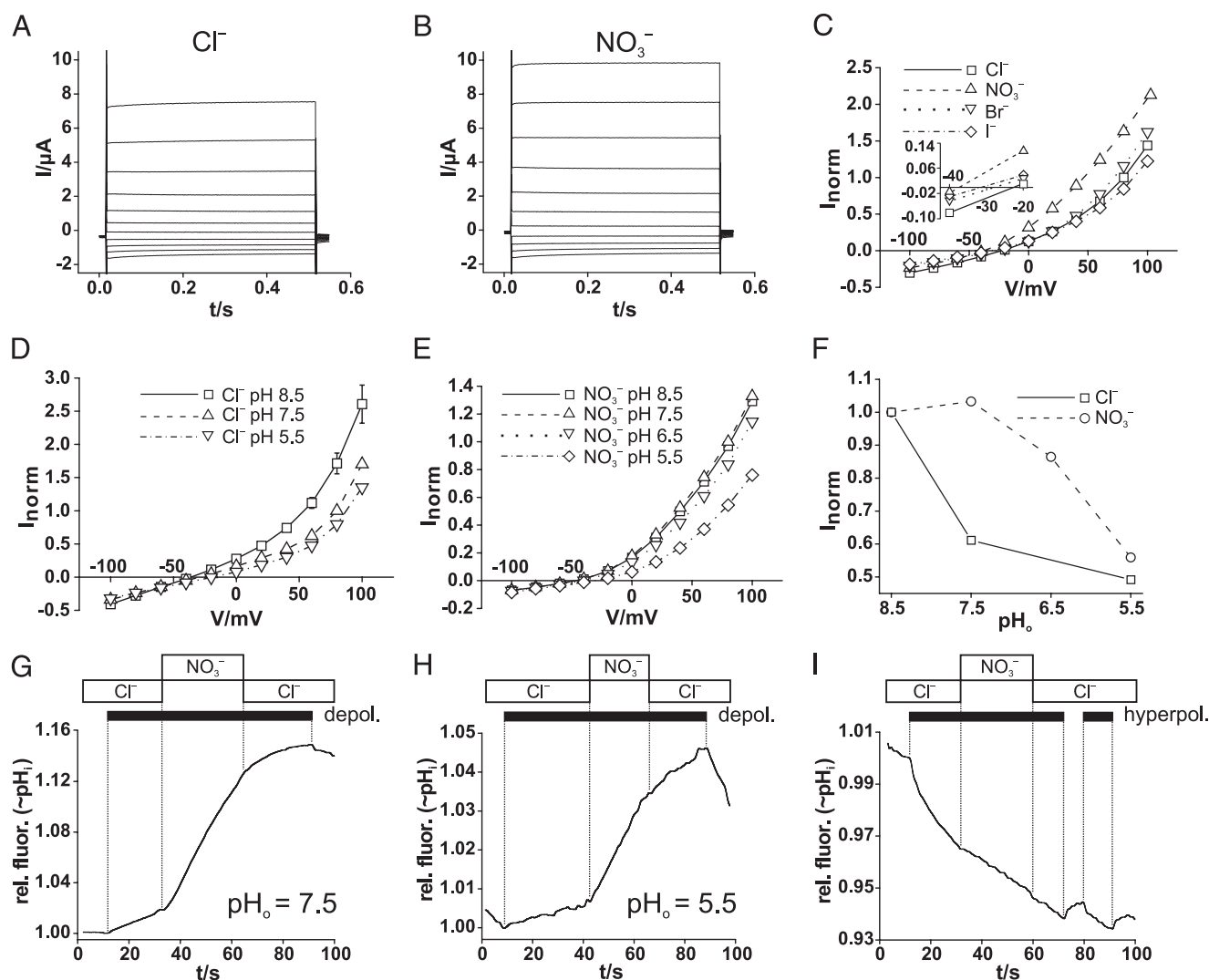


FIGURE 1. Electrophysiological characterization of AtClC-a in *Xenopus* oocytes. *A* and *B*, voltage-clamp traces of oocyte-expressed AtClC-a in either Cl^- -containing (*A*) or NO_3^- -containing (*B*) solutions. From a holding potential of -30 mV, the oocyte was clamped in 20-mV steps to voltages between -100 and $+100$ mV for 500 ms. *C*, steady-state I/V curves of AtClC-a with different extracellular anions. Currents were normalized for individual oocytes to a current at $+80$ mV in Cl^- solution (with a mean value of $3.38 \pm 0.40 \mu\text{A}$). AtClC-a has a $\text{NO}_3^- > \text{Br}^- > \text{Cl}^- > \text{I}^-$ conductance sequence (mean values from 13 oocytes from four batches; error bars, S.E.). *Inset*, higher magnification of the I/V curve to show reversal potentials. *D* and *E*, steady-state I/V curves of AtClC-a at different values of extracellular pH (pH_o) in Cl^- -containing (*D*) or NO_3^- -containing (*E*) solutions. The voltage-clamp protocol was performed as in *A* and *B*. Currents were normalized for individual oocytes to the respective current at $+80$ mV at pH_o 7.5 (five oocytes for each data point; error bars, S.E.). *F*, currents at $+80$ mV as a function of pH_o with extracellular Cl^- (\square) or NO_3^- (\circ). For each curve, currents were normalized to currents at pH_o 8.5. *G–I*, AtClC-a mediated, voltage-driven H^+ transport assayed by pH-sensitive BCECF fluorescence using the Fluorocyte system (21). Proton transport was stimulated by trains (black bars) of 400-ms long voltage pulses, either to $+90$ mV (depolarization) in (*G* and *H*) or to -160 mV (hyperpolarization) in *I* in the presence of either extracellular Cl^- or NO_3^- (shown in boxes above). Depolarizing pulses elicited intracellular alkalinization both with pH_o 7.5 (*G*) and pH_o 5.5, when proton transport occurs against a gradient (*H*). Extracellular NO_3^- accelerates depolarization (*depol.*)-driven alkalinization (*G* and *H*) but not hyperpolarization (*hyperpol.*)-induced acidification (*I*, pH_o 7.5). Only changes in relative fluorescence (*rel. fluor.*) induced by changes in voltage or external anions are relevant because of the drift inherent to the Fluorocyte technique (21). Results as in *G–I* were obtained in 26, 6, and 7 independent experiments, respectively.

port (17, 19, 20). In crystals of the bacterial protein, the negatively charged side chain of this glutamate seems to block the permeation pathway (22, 23). Mutating this glutamate to alanine in ClC-4 and -5 not only leads to flux uncoupling but also abolishes the strong outward rectification of either transporter (26). Likewise, currents of the E203A mutant lost their outward rectification (Fig. 2). Rather than being linear and again similar to the analogous mutants of ClC-4 and -5 (19, 20, 26), currents showed slight outward rectification at positive voltages and slight inward rectification at negative voltages. Contrasting with the moderate changes in ion selectivity observed with such mutations in ClC-4 and -5 (26), the E203A mutation drastically

altered the anion selectivity of AtClC-a. Whereas reversal potentials indicated that the mutant remained more permeable for NO_3^- than for Cl^- (Fig. 2*C*, *inset*), its conductance was now reduced rather than increased when extracellular Cl^- was replaced by NO_3^- (Fig. 2, *A–C*; see Fig. 4*F*). With either external anion, currents were insensitive to changes in pH_o (Fig. 2, *D* and *E*), and trains of depolarizing pulses failed to change pH_i (Fig. 2*F*). Hence, the E203A mutant displayed uncoupled anion transport and drastically reduced conductance in the presence of NO_3^- .

We next studied the AtClC-a mutant E270A, which is equivalent to the proton glutamate mutations of EcClC-1 (27) and

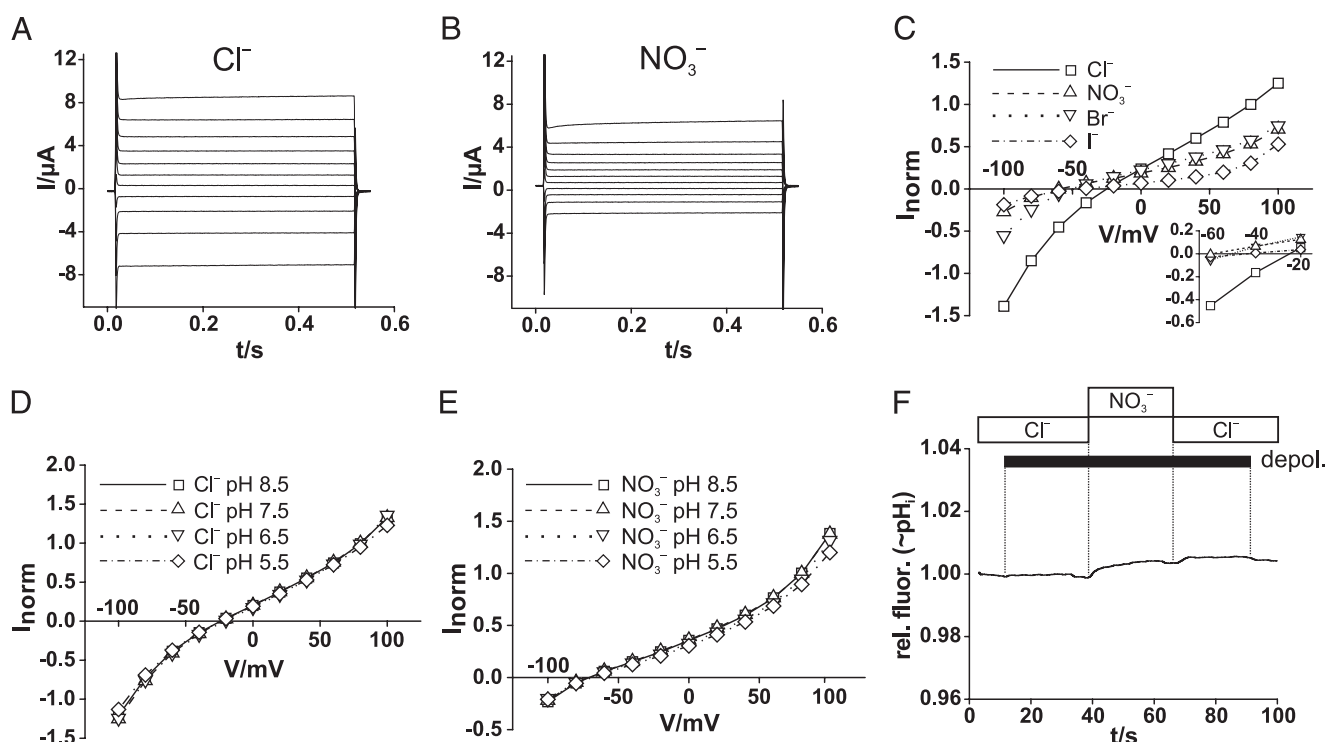


FIGURE 2. Impact of gating glutamate mutant E203A on AtClC-a properties. *A* and *B*, voltage-clamp traces of oocytes expressing the E203A mutant of AtClC-a with extracellular Cl^- (*A*) or NO_3^- (*B*) using the pulse protocol of Fig. 1 (*A* and *B*). *C*, steady-state I/V curves of AtClC-a(E203A) with different extracellular anions reveal a changed conductance sequence of $\text{Cl}^- > \text{Br}^- > \text{NO}_3^- > \text{I}^-$ (mean of 19 oocytes; error bars, S.E.). Currents were normalized to current in Cl^- at +80 mV (with mean current of $3.05 \pm 0.22 \mu\text{A}$). *Inset*, higher magnification of the I/V curve to show reversal potentials. *D* and *E*, currents of AtClC-a(E203A) are insensitive to pH_o , both in the presence of extracellular Cl^- (*D*) or NO_3^- (*E*). The number of oocytes is 10 for *D* and 14 for *E* (error bars, S.E.). *F*, lack of depolarization (*depol.*)-induced alkalinization with the E203A mutant. 25 independent experiments gave similar results. *rel. fluor.*, relative fluorescence.

ClC-4 and -5 (Fig. 3) (21). Neither currents (Fig. 3, *A–C*) nor depolarization-induced H^+ transport (Fig. 3, *G* and *H*) were different from background levels with this mutant. However, when combined with the uncoupling E203A mutation in the gating glutamate, the AtClC-a(E203A,E270A) double mutant gave currents that resembled those of the single E203A mutant (Fig. 3, *D–F*). Like AtClC-a(E203A), the double mutant failed to transport protons in response to depolarization (Fig. 3*I*).

Two main biophysical differences between AtClC-a and ClC-4 and -5 are (i) the much stronger rectification of the mammalian isoforms and (ii) their partial uncoupling of anion from proton transport in the case of nitrate. We therefore searched for differences in their primary sequences that may underlie these differences. A salient feature is the presence of a proline in a stretch of highly conserved “signature” sequences (Fig. 4*A*). In AtClC-a, this proline replaces a serine that is found at this position in most CLC proteins. The importance of that serine was recognized early on (25). Even the conservative exchange of this serine for threonine (S123T) changed the ion selectivity, single-channel conductance, and open-channel rectification of the ClC-0 Cl^- channel (25). In the crystal of EcClC-1, the equivalent serine (Ser-107) participates in the coordination of Cl^- in the central binding site (22). Mutating this particular proline in AtClC-a to the “consensus” serine (P160S) resulted in less rectifying currents (Fig. 4, *B–D*), indicating that the difference in rectification between WT AtClC-a and ClC-5 proteins is not determined by the residue at this position. Importantly, both the apparent permeability (from reversal potentials) and conductance no longer differed measurably between NO_3^- and Cl^-

solutions (Fig. 4, *B–D*). Furthermore, the mutant performed Cl^-/H^+ - and NO_3^-/H^+ exchange with similar efficiencies (Fig. 4*E*). When this proline was mutated to glycine (P160G), the ratio of currents measured in the presence of extracellular NO_3^- ($I(\text{NO}_3^-)$) to those measured with extracellular Cl^- ($I(\text{Cl}^-)$) resembled the ratio $I(\text{NO}_3^-)/I(\text{Cl}^-)$ of WT AtClC-a (Fig. 4*F*), with which it also shares the higher efficiency of NO_3^-/H^+ exchange as compared with Cl^-/H^+ exchange (data not shown). When the P160S mutation was combined with the uncoupling mutation in the gating glutamate, the resulting double mutant AtClC-a(P160S,E203A) displayed a low $I(\text{NO}_3^-)/I(\text{Cl}^-)$ ratio that was similar to the single E203A mutant (Fig. 4*F*) and had lost proton coupling (data not shown).

The above experiments indicate that the presence of proline in the CLC signature sequence may be responsible for the efficient NO_3^-/H^+ coupling of AtClC-a. We asked next whether changing the equivalent serine to proline in ClC-5 would increase its efficiency of NO_3^-/H^+ coupling. In the presence of extracellular chloride, currents from the ClC-5(S168P) mutant (Fig. 5*D*) were much smaller (~ 5 – 10 -fold) than WT currents (Fig. 5*A*). They increased ~ 3 -fold in the presence of extracellular NO_3^- (Fig. 5*E*), coinciding with the recent parallel work by Zifarelli and Pusch (38). Whereas currents of WT ClC-5 are also larger with NO_3^- than with Cl^- (Fig. 5, *A–C*), the $I(\text{NO}_3^-)/I(\text{Cl}^-)$ ratio is markedly increased in the mutant (Fig. 5, *D–F* and *K*). The strong rectification of ClC-5 currents is not appreciably affected by the S168P mutation (Fig. 5, *A–F*), but currents showed somewhat more pronounced and slower “gating” relaxations when jumping to positive voltages. In contrast to WT

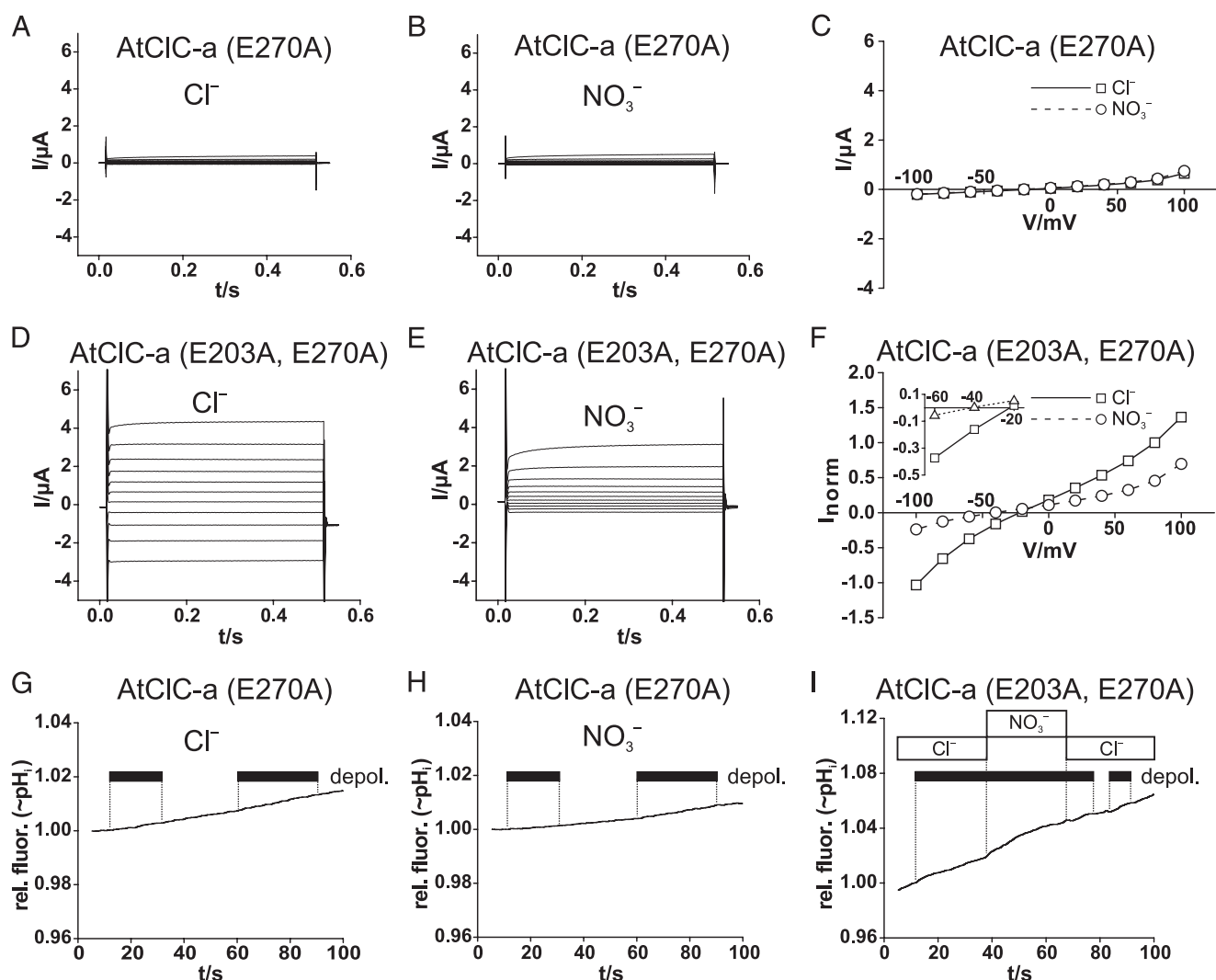


FIGURE 3. Effect of proton glutamate E270A mutation alone and in combination with the uncoupling E203A mutation on AtCIC-a transport. *A* and *B*, voltage-clamp traces of oocyte-expressed AtCIC-a(E270A) in either Cl^- -containing (*A*) or NO_3^- -containing (*B*) solutions are not different from those from uninjected control oocytes (not shown). *C*, steady-state I/V curves of AtCIC-a(E270A) are not different from controls (10 oocytes per data point). Currents were normalized to current at +80 mV in Cl^- . *D* and *E*, currents of the AtCIC-a(E203A,E270A) double mutant are larger with Cl^- (*D*) than with NO_3^- (*E*). These results also suggest that the failure to observe AtCIC-a(E270A) currents is not due to an absence from the plasma membrane. *F*, I/V curves of currents averaged from nine oocytes from four batches are shown. Currents were normalized to those in Cl^- at 80 mV (with mean current of $1.86 \pm 0.47 \mu\text{A}$). *Inset*, a higher magnification of the I/V curve shows reversal potentials. *G* and *H*, shown is a lack of detectable depolarization (*depol.*)-induced alkalinization with AtCIC-a(E270A) in the presence of Cl^- (*G*) or NO_3^- (*H*). Similar negative results were obtained with nine oocytes (from four batches) for *G* and *H*. *I*, shown is a lack of depolarization-induced proton transport with AtCIC-a(E203A,E270A). Similar results were obtained with five oocytes from three batches. Voltage-clamp protocols are identical to those described in the legend to Fig. 1. *rel. fluor.*, relative fluorescence.

CIC-5 (Fig. 5G), trains of depolarizing pulses alkalinized the oocyte interior much more rapidly when extracellular Cl^- was replaced by NO_3^- (Fig. 5J). CIC-5(S168P) transported H^+ efficiently against its electrochemical gradient (with pH_o 5.5) using NO_3^- as a driving ion (Fig. 5J). When Ser-168 of CIC-5 was replaced by glycine or alanine, only the S168A mutation yielded a moderately higher $I(\text{NO}_3^-)/I(\text{Cl}^-)$ current ratio (Fig. 5K). This contrasts with AtCIC-a, where glycine could substitute for proline without compromising its $I(\text{NO}_3^-)/I(\text{Cl}^-)$ ratio (Fig. 4K) and its efficient NO_3^-/H^+ exchange. Hence, a single mutation that replaced a serine by proline, which is found at that position in AtCIC-a, strongly increased the preference of CIC-5 for NO_3^- and converted it into an efficient NO_3^-/H^+ exchanger.

The uncoupling E211A mutation in the CIC-5 gating glutamate slightly increased its relative nitrate conductance (Fig.

5K), whereas the equivalent mutation in AtCIC-a quite drastically lowered its nitrate *versus* chloride conductance (Fig. 4F). Exchanging serine 168 for proline in the uncoupled CIC-5 mutant increased relative conductance in the presence of NO_3^- (Fig. 5K), whereas a similar exchange in the uncoupled AtCIC-a mutant failed to change the $I(\text{NO}_3^-)/I(\text{Cl}^-)$ current ratio (Fig. 4F).

We finally asked whether also CLC Cl^- channels gain higher NO_3^- conductance with an equivalent mutation and used the *Torpedo* Cl^- channel CIC-0 (35) as a widely used model channel. When expressed in *Xenopus* oocytes, the S123P mutant gave robust currents that were, however, ~ 4 -fold smaller than those from WT CIC-0 (Fig. 6, *A* and *D*). Whereas the WT channel conducts Cl^- much better than nitrate (Fig. 6, *A*–*C*), NO_3^- conductance was larger than Cl^- conductance in the S123P

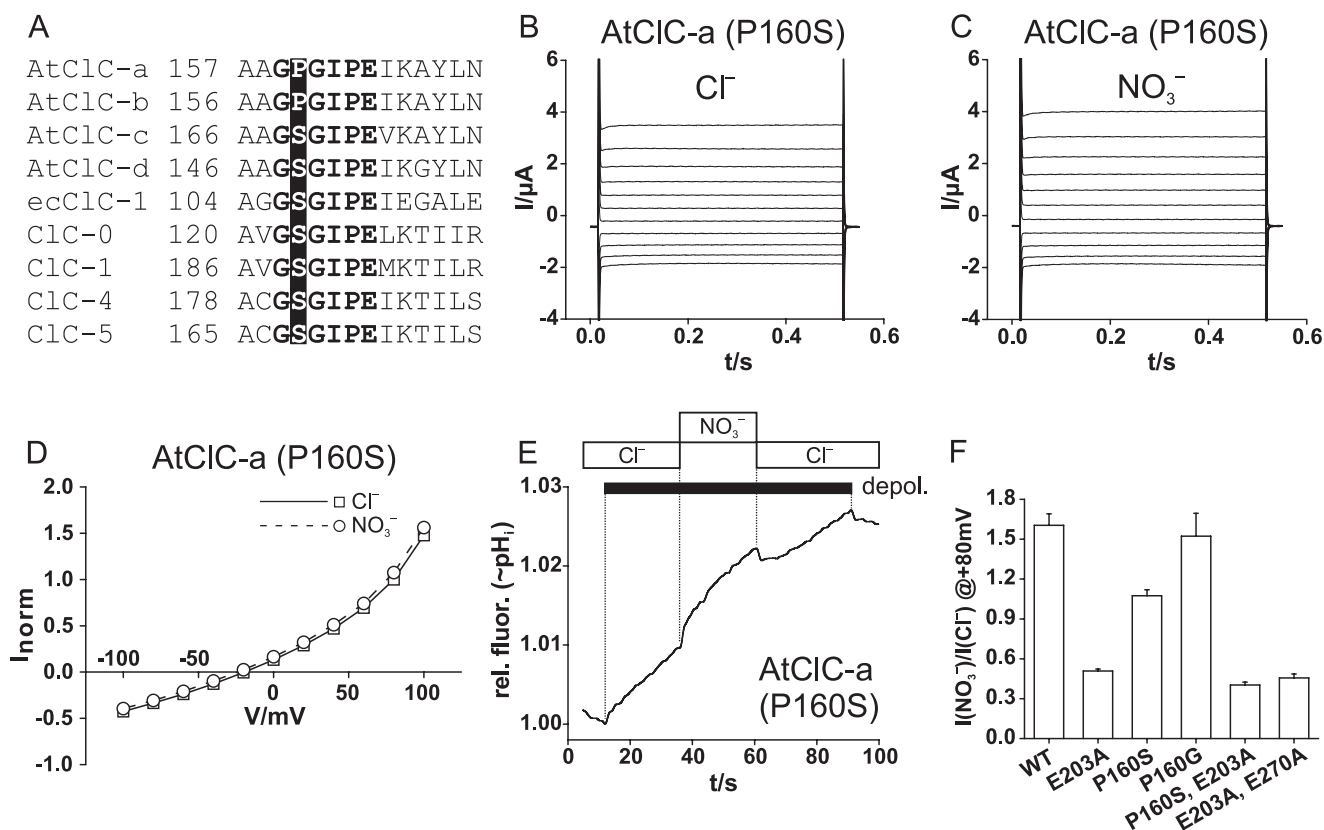


FIGURE 4. A critical role of proline residue in AtClC-a in determining anion selectivity. *A*, shown is the sequence alignment of several CLC proteins in the region of the GSGIPE signature sequence. *E. coli* EcClC-1 as well as all animal CLC proteins have a serine between the two glycines. It is replaced by proline in plant AtClC-a and -b, but not in AtClC-c and -d. *B* and *C*, shown are typical two-electrode voltage-clamp traces of the AtClC-a P160S mutant in *Xenopus* oocytes with external Cl^- (*B*) or NO_3^- (*C*) (voltage protocol as in Fig. 1). *D*, the current-voltage relationship of the mutant appears to be identical in extracellular Cl^- and NO_3^- (mean of nine oocytes from six batches each). Currents were normalized to those in Cl^- at +80 mV (where mean current was $2.33 \pm 0.44 \mu\text{A}$). *E*, depolarization (*depol.*)-induced H^+ transport of AtClC-a (P160S) is similarly effective with extracellular Cl^- or NO_3^- , in stark contrast to the WT (Fig. 1*G,H*). Similar results were obtained in 14 experiments (14 oocytes from six batches). *F*, shown is the ratio of currents at +80 mV in the presence of NO_3^- and Cl^- for AtClC-a and several mutants, respectively. The number of oocytes is as follows: AtClC-a, 25; AtClC-a(E203A), 24; AtClC-a(P160S), 9; AtClC-a(P160G), 5; AtClC-a(P160S,E203A), 4; and AtClC-a(E203A,E270A), 9. *rel. fluor.*, relative fluorescence.

mutant (Fig. 6, *D–F*). The selectivity was also changed for other anions, as evident in the large increase of Br^- conductance (Fig. 6*F*). In addition, the mutation drastically slowed the fast protopore gate (as evident from current relaxations after stepping to negative voltages, Fig. 6, *A* and *D*) and introduced an open-pore outward rectification (Fig. 6, *C* and *F*). The concomitant change of pore and gating properties reflects the tight coupling of permeation and gating in CLC Cl^- channels (39).

DISCUSSION

We have achieved for the first time the functional expression of a plant CLC transporter in animal cells. This enabled us to study the currents and proton transport of wild-type and mutant AtClC-a, a NO_3^-/H^+ exchanger that serves to accumulate the plant nutrient NO_3^- in vacuoles (16, 37). We have studied the role in AtClC-a of key glutamate residues that are important for anion/proton coupling in bacterial and mammalian CLC isoforms and have shown that a proline-serine exchange in a highly conserved stretch (GSGIPE, the “CLC signature sequence”) strongly affects nitrate/proton transport in AtClC-a and ClC-5.

In our previous study, we were unable to detect plasma membrane currents in *Xenopus* oocytes injected with AtClC-a–AtClC-d (12). Currents reported previously for the oocyte-ex-

pressed tobacco CLC NtClC (40) resemble endogenous oocyte currents (12). Hence, the present study may represent the first functional characterization of plant CLC proteins in animal cells. This renders AtClC-a accessible to structure-function analysis by mutagenesis. The most important technical differences from our previous study (12) are the injection of about twice the amount of RNA and a longer time of expression. Whereas we previously measured oocytes 3 days after injection, we now found that AtClC-a currents rise above background levels only after 5 days. Because AtClC-a is physiologically expressed in the plant vacuole (16), the presence of plasma membrane currents may indicate a misrouting of AtClC-a in overexpressing oocytes.

The currents reported here for oocyte-expressed AtClC-a resemble in many aspects the currents from *Arabidopsis* vacuoles that were studied by patch clamp in the whole vacuole configuration and that were absent in strains with AtClC-a gene deletions (16). Both currents showed similar rectification and proton coupling. However, there are also conspicuous differences. When studied under asymmetric ionic conditions with NO_3^- in the pipette (vacuole) and Cl^- in the bath (cytosol), which resembles our oocyte experiments with external NO_3^- , vacuolar currents showed prominent, depolarization-induced

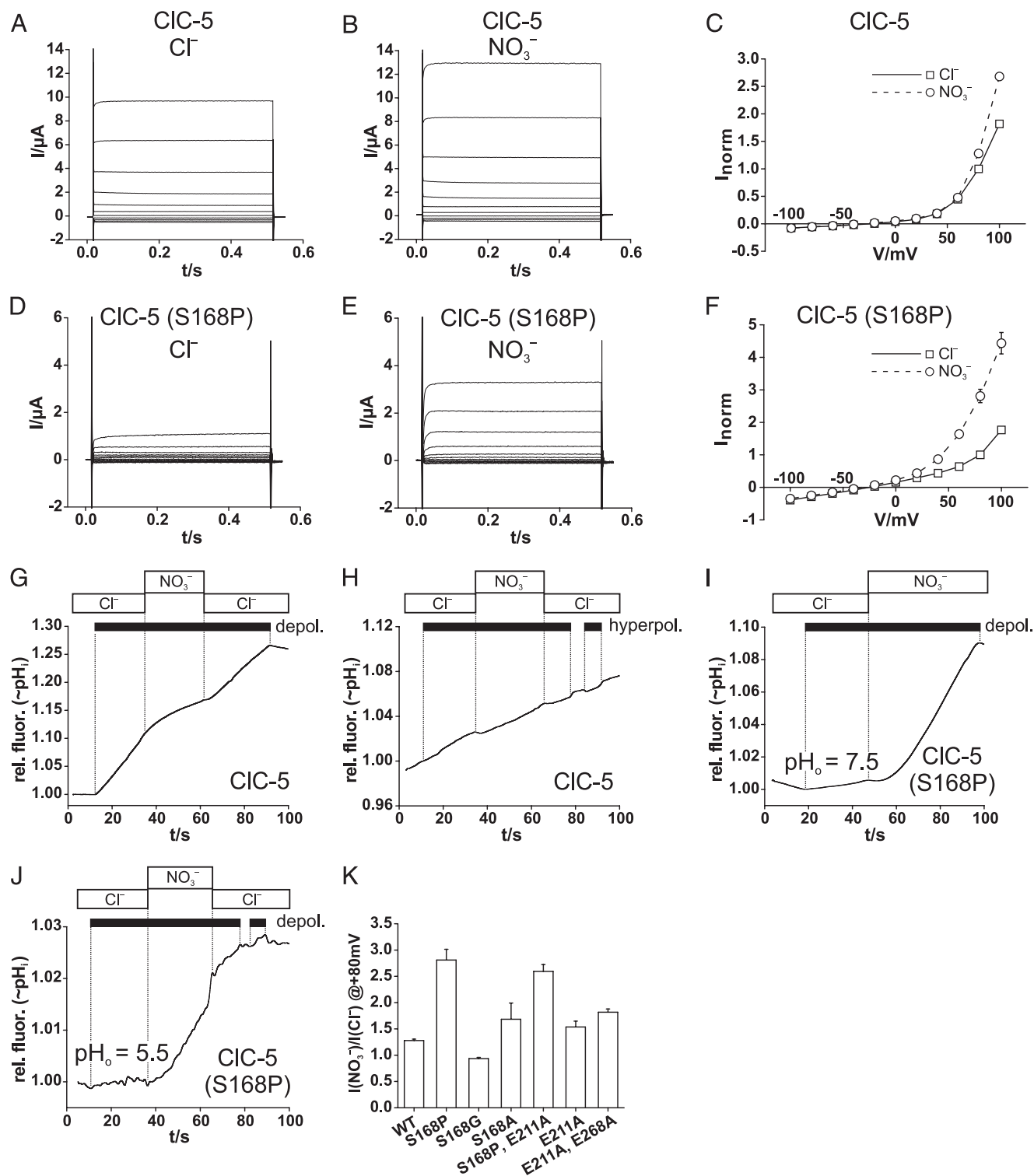


FIGURE 5. Effect of the S168P mutation on CIC-5 conductance and proton coupling. A and B, shown are the typical two-electrode voltage-clamp traces of oocyte-expressed CIC-5 in Cl^- -containing (A) or NO_3^- -containing (B) solutions. C, shown are the steady-state I/V curves from such experiments (averaged from 19 oocytes from seven batches; normalized for each oocyte to current in Cl^- at +80 mV, with mean current of $3.01 \pm 0.35 \mu\text{A}$). D–F, shown are the current properties of the S168P mutant measured as in A–C. The data in F show means from 23 oocytes from five batches, normalized to I in Cl^- at +80 mV, with mean I of $0.79 \pm 0.17 \mu\text{A}$. Voltage-clamp protocols were performed in A–F as described in the legend to Fig. 1. G, shown is an example of less efficient depolarization (depol.)-induced alkalinization by CIC-5 in the presence of NO_3^- compared with Cl^- . Similar results were obtained in 17 experiments. H, hyperpolarization (hyperpol.) does not elicit intracellular acidification with CIC-5, in contrast to AtCIC-a (Fig. 1). Similar results were obtained in 13 experiments. I and J, shown is the drastically increased NO_3^-/H^+ exchange activity with CIC-5 (S168P), as shown by Fluorocyt with pH_o 7.5 (I) or with pH_o 5.5 (transport against gradient) (J), resembling in this respect AtCIC-a (Fig. 1G and H). Similar results were obtained in 21 (I) and eight (J) experiments. K, shown is a ratio of currents at +80 mV measured with extracellular NO_3^- and Cl^- , respectively, for CIC-5 and several mutants, determined as in Fig. 4F. The number of oocytes used for averages are as follows: CIC-5, 19; CIC-5(S168P), 23; CIC-5(S168G), 17; CIC-5(S168A), 2; CIC-5(S168P,E211A), 6; CIC-5(E211A), 10; CIC-5(E211A,E268A), 34). Error bars indicate S.E. rel. fluor., relative fluorescence.

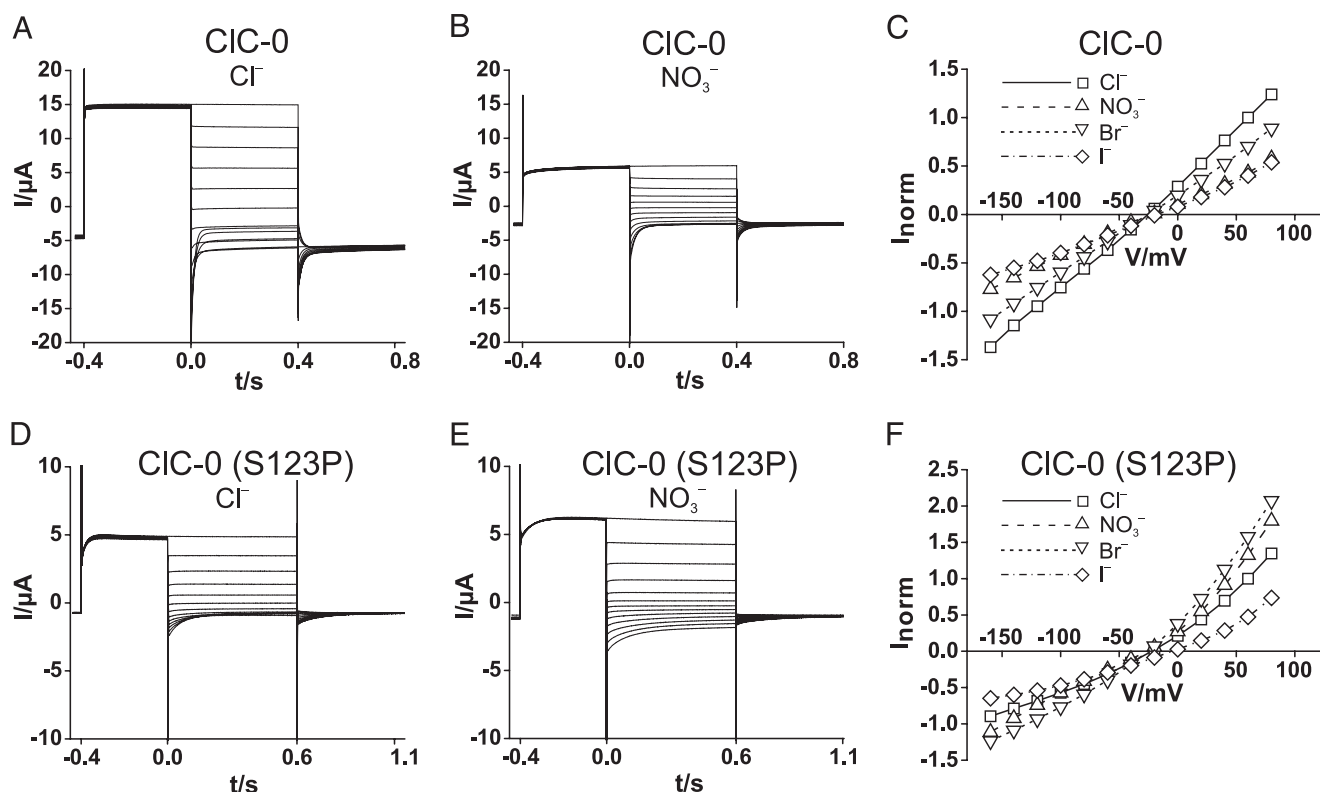


FIGURE 6. Modification of CIC-0 Cl^- channel currents by the S123P mutation. *A* and *B*, typical voltage-clamp traces of an oocyte expressing WT CIC-0 and measured in Cl^- saline (*A*) and NO_3^- saline (*B*). After ~ 8 s at -120 mV (to activate the slow hyperpolarization-activated gate of CIC-0), the oocytes were clamped consecutively for 1 s to -120 mV (to keep the "slow" common gate open), 400 ms to $+80$ mV to open the fast protopore gate. At $t = 0$, they were clamped (for 400 ms) to test voltages between $+80$ and -160 mV in steps of 20 mV, followed by a constant pulse to -100 mV for 400 ms. *C*, normalized I/V curves of WT CIC-0 in the presence of different extracellular anions. Values were obtained from exponential fits to $t = 0$ and represent open channel currents because both slow and fast gates were opened by hyperpolarizing and depolarizing prepulses, respectively. Averaged currents from five oocytes of two batches were normalized for each individual oocyte to the current in Cl^- at $V = +60$ mV, where mean I was $13.8 \pm 2.2 \mu\text{A}$. *D* and *E*, typical traces from an oocyte expressing the S123P mutant of CIC-0. Voltage-clamp protocol was similar to *A*, but the test voltages were applied for 600 ms, followed by a 500-ms pulse to -100 mV. *F*, normalized open-channel I/V for the mutant obtained as in *C*. Means are from seven oocytes of two batches (normalized to current in Cl^- at $+60$ mV, where mean I was $4.41 \pm 0.90 \mu\text{A}$).

activation that remained incomplete after several seconds (16). Such current relaxations were clearly absent from our recordings. Moreover, whereas our currents increased with extracellular NO_3^- only ~ 1.6 -fold, this increase was much more drastic with vacuolar currents (16). Several explanations may be invoked. Current properties may be influenced by different lipid compositions of membranes from oocytes and plant vacuoles, or AtCIC-a might endogenously form complexes with other proteins. These other proteins may include structurally unrelated ancillary β -subunits (as known for some mammalian CLC proteins) (10, 41), other AtCIC isoforms (12) (CLC proteins function as dimers (22, 25, 30)), or anchoring proteins.

The outward rectification of AtCIC-a is less strong than that of CIC-4 and -5, both of which do not transport measurably at negative voltages (26). This difference is not due to the presence of proline instead of serine in the signature sequence of AtCIC-a, as revealed by our mutagenesis experiments. The weaker rectification of AtCIC-a may be crucial for the proton-driven uptake of NO_3^- into vacuoles that may have a lumen-positive voltage. The much stronger rectification of CIC-4 and -5 is *a priori* difficult to reconcile with their presumed role in electrical compensation of H^+ -ATPase currents (11).

The heterologous expression of AtCIC-a allowed the first structure-function analysis of a plant CLC protein. We began

by studying two glutamate residues that are conserved in all confirmed CLC exchangers. The gating glutamate is important for anion/proton coupling in CLC exchangers, as well as for gating in CLC Cl^- channels. Its replacement in AtCIC-a by alanine uncoupled anion flux from protons as in other CLC transporters (17, 21). Similar to CIC-4 and CIC-5, this mutation also drastically changed current rectification, with both inward and outward rectification being observed. Unlike equivalent mutations in CIC-4 and -5, this uncoupling AtCIC-a mutation also drastically changed the $I(\text{NO}_3^-)/I(\text{Cl}^-)$ current ratio. This change did not depend on the presence of a proline in the signature sequence.

In CLC anion/proton exchangers, the pathways of Cl^- and H^+ diverge at a point approximately half-way through the membrane and reach the cytoplasm at different points (27). A proton glutamate at the cytoplasmic CLC surface is thought to bind protons, handing them over to the gating glutamate using a poorly defined path. In both mammalian and *E. coli* CLC exchangers, this glutamate could be replaced by other titratable amino acids without abolishing anion/proton coupling (21, 27, 42). When mutated to nontitratable residues, however, Cl^- and H^+ transport were below detection levels in CIC-4 and -5 (21), whereas small, uncoupled anion currents were observed with EcCIC-1 (42). This can be rationalized by a blockade of anion/

proton exchange at the gating glutamate, when the supply of protons ceases (21). The uncoupled but reduced anion flux in EcCLC-1 might be owed to “slippage” past the central exchange site (42). This model is strongly supported by double mutants in CLC-4 and -5, in which the uncoupling gating glutamate mutation rescued the uncoupled anion flux (21). Exactly this situation was found here with AtCLC-a.

It was puzzling that anion transport of CLC-4, -5, and EcCLC-1 is largely uncoupled from proton transport with the polyatomic anion NO_3^- (21), whereas AtCLC-a efficiently couples NO_3^- to proton countertransport (16), an essential property for its role in accumulating this plant nutrient in vacuoles. Using sequence comparison, we identified a proline in the CLC signature sequence as a likely candidate for this difference. In all animal CLC proteins, this position is occupied by serine. Indeed, when Pro-160 in AtCLC-a was mutated to serine, the plant transporter performed the Cl^-/H^+ exchange with similar efficiency as the NO_3^-/H^+ exchange, rather than preferring NO_3^- as in the WT. Importantly, when the equivalent serine of CLC-5 was mutated to proline, CLC-5 mediated an efficient NO_3^-/H^+ exchange both in the present study as well as in parallel work by Zifarelli and Pusch (38). A novel method (43) to measure proton transport allowed these authors to show that CLC-5(S168P) had gained an NO_3^-/H^+ coupling ratio of ~ 2 at voltages between +40 and +60 mV, indistinguishable from that for Cl^-/H^+ exchange (38). Our data on other CLC-5 mutants at this position (Fig. 5K) largely agree with their results (38) but show interesting differences with data obtained for AtCLC-a (Fig. 4F). The substitution of the critical proline by glycine in AtCLC-a did not interfere with its efficient NO_3^-/H^+ exchange, possibly suggesting that a helix breaker might be sufficient to support such an exchange. However, glycine at the equivalent position in CLC-5 does not increase currents in the presence of NO_3^- nor does it enable efficient NO_3^-/H^+ exchange (data not shown) (38).

Only four of seven *Arabidopsis* CLC proteins have a proline in their signature sequence, with the remaining three displaying a serine like all known animal CLC proteins. This suggests that all these four proline-containing AtCLC proteins function as $2\text{NO}_3^-/\text{H}^+$ exchangers. A more definitive assignment of their physiological roles, however, is not yet possible. In this respect, it is interesting to note that only AtCLC-c and AtCLC-d were reported to complement (12, 32) growth phenotypes of a *Saccharomyces cerevisiae* strain deleted for the single yeast CLC (ScCLC or Gef) (33). Whether this is related to the fact that AtCLC-c and -d, just like ScCLC, carry serine in their signature sequence and hence probably prefer chloride over nitrate remains unclear.

The interpretation of conductance ratios of CLC-5, and by extension of AtCLC-a, is complicated by results from a noise analysis that indicates that CLC-5 switches from transporting to nontransporting modes of operation (21). Such a gating of transport activity probably underlies the time-dependent current relaxation upon depolarization of CLC-5 and might also explain the slow depolarization-induced activation of vacuolar currents observed by De Angeli *et al.* (16). Zifarelli and Pusch (38) recently concluded from their noise analysis that the increase in CLC-5 currents with NO_3^- is not due to an increased

“unitary conductance” of the “turned on” transporter (which would include slippage of the anion) but rather to a higher “open probability” of the transporter. However, it seems unlikely that the difference in $I(\text{NO}_3^-)/I(\text{Cl}^-)$ ratios between WT AtCLC-a and mutant P160S is solely due to an effect on gating. This is because this mutation not only modified conductance ratios but also changed the apparent permeability (reversal potentials). We therefore conclude that the proline-serine exchange affects the ion selectivity of the exchange process. This conclusion is indirectly bolstered by the single-channel analysis of the CLC-0(S123T) mutant, which demonstrated changes in ion selectivity and other pore properties (25) and by the changed ion selectivity of the CLC-0(S123P) mutant described here. Unfortunately, we cannot draw similar conclusions for CLC-5 because its strong rectification precludes the determination of reversal potentials.

In the crystal of EcCLC-1, the equivalent serine participates in the coordination of a Br^- ion (used as a Cl^- substitute in crystallography) in the central binding site (22). Several mutations in Tyr-445, another residue involved in this coordination (22), uncoupled chloride from proton fluxes (44). Such mutations were associated with a reduced presence or complete absence of anions at the central binding site (44). Likewise, crystals obtained in the presence of NO_3^- revealed that this anion, which uncouples Cl^- from H^+ transport in EcCLC-1, cannot be detected at this position (18). Thus, anion/proton coupling seems to require that an anion occupies this site. It was proposed that this anion serves as an intermediate binding site for protons on their way from the proton glutamate to the gating glutamate, leading to the seemingly outlandish proposal of HCl as a proton transport intermediate (45). We suggest that the replacement of serine by proline in the GSGIPE sequence enables NO_3^- to occupy the central anion binding site, thereby leading to efficient proton coupling.

In summary, a breakthrough in heterologous expression of AtCLC-a has allowed us to extend the structure-function analysis of anion/proton exchange to plant CLC proteins. Mutagenesis of critical gating and proton glutamates resulted in changes of proton coupling and rectification that bear close resemblance to results from mammalian endosomal CLC proteins. However, there were also significant differences in effects on NO_3^- conductance. We further identified an important proline residue in the CLC signature sequence of AtCLC-a that is crucial for its efficient NO_3^-/H^+ exchange activity and that conferred more efficient NO_3^-/H^+ coupling on the mammalian CLC-5 exchanger and an increase in NO_3^- conductance on the *Torpedo* Cl^- channel CLC-0. Our work provides a basis for future studies of other plant CLC proteins and their comparison to mammalian counterparts.

Acknowledgments—We thank A. Fast, N. Kroenke, P. Seidler, and S. Zillmann for technical assistance.

REFERENCES

- Jentsch, T. J. (2008) *Crit. Rev. Biochem. Mol. Biol.* **43**, 3–36
- Bösl, M. R., Stein, V., Hübner, C., Zdebik, A. A., Jordt, S. E., Mukhopadhyay, A. K., Davidoff, M. S., Holstein, A. F., and Jentsch, T. J. (2001) *EMBO J.* **20**, 1289–1299

3. Simon, D. B., Bindra, R. S., Mansfield, T. A., Nelson-Williams, C., Mendonca, E., Stone, R., Schurman, S., Nayir, A., Alpay, H., Bakkaloglu, A., Rodriguez-Soriano, J., Morales, J. M., Sanjad, S. A., Taylor, C. M., Pilz, D., Brem, A., Trachtman, H., Griswold, W., Richard, G. A., John, E., and Lifton, R. P. (1997) *Nat. Genet.* **17**, 171–178
4. Matsumura, Y., Uchida, S., Kondo, Y., Miyazaki, H., Ko, S. B., Hayama, A., Morimoto, T., Liu, W., Arisawa, M., Sasaki, S., and Marumo, F. (1999) *Nat. Genet.* **21**, 95–98
5. Rickheit, G., Maier, H., Strenzke, N., Andreescu, C. E., De Zeeuw, C. I., Muenscher, A., Zdebik, A. A., and Jentsch, T. J. (2008) *EMBO J.* **27**, 2907–2917
6. Steinmeyer, K., Klocke, R., Ortland, C., Gronemeier, M., Jockusch, H., Gründer, S., and Jentsch, T. J. (1991) *Nature* **354**, 304–308
7. Piwon, N., Günther, W., Schwake, M., Bösl, M. R., and Jentsch, T. J. (2000) *Nature* **408**, 369–373
8. Kornak, U., Kasper, D., Bösl, M. R., Kaiser, E., Schweizer, M., Schulz, A., Friedrich, W., Delling, G., and Jentsch, T. J. (2001) *Cell* **104**, 205–215
9. Kasper, D., Planells-Cases, R., Fuhrmann, J. C., Scheel, O., Zeitz, O., Ruether, K., Schmitt, A., Poët, M., Steinfeld, R., Schweizer, M., Kornak, U., and Jentsch, T. J. (2005) *EMBO J.* **24**, 1079–1091
10. Lange, P. F., Wartosch, L., Jentsch, T. J., and Fuhrmann, J. C. (2006) *Nature* **440**, 220–223
11. Jentsch, T. J. (2007) *J. Physiol. (Lond.)* **578**, 633–640
12. Hechenberger, M., Schwappach, B., Fischer, W. N., Frommer, W. B., Jentsch, T. J., and Steinmeyer, K. (1996) *J. Biol. Chem.* **271**, 33632–33638
13. Marmagne, A., Vinauger-Douard, M., Monachello, D., de Longevialle, A. F., Charon, C., Allot, M., Rappaport, F., Wollman, F. A., Barbier-Brygoo, H., and Ephritikhine, G. (2007) *J. Exp. Bot.* **58**, 3385–3393
14. von der Fecht-Bartenbach, J., Bogner, M., Krebs, M., Stierhof, Y. D., Schumacher, K., and Ludewig, U. (2007) *Plant J.* **50**, 466–474
15. De Angeli, A., Monachello, D., Ephritikhine, G., Frachisse, J. M., Thomine, S., Gambale, F., and Barbier-Brygoo, H. (2009) *Philos. Trans. R. Soc. Lond. B Biol. Sci.* **364**, 195–201
16. De Angeli, A., Monachello, D., Ephritikhine, G., Frachisse, J. M., Thomine, S., Gambale, F., and Barbier-Brygoo, H. (2006) *Nature* **442**, 939–942
17. Accardi, A., and Miller, C. (2004) *Nature* **427**, 803–807
18. Nguitrageol, W., and Miller, C. (2006) *J. Mol. Biol.* **362**, 682–690
19. Scheel, O., Zdebik, A., Lourdel, S., and Jentsch, T. J. (2005) *Nature* **436**, 424–427
20. Picollo, A., and Pusch, M. (2005) *Nature* **436**, 420–423
21. Zdebik, A. A., Zifarelli, G., Bergsdorf, E.-Y., Soliani, P., Scheel, O., Jentsch, T. J., and Pusch, M. (2008) *J. Biol. Chem.* **283**, 4219–4227
22. Dutzler, R., Campbell, E. B., Cadene, M., Chait, B. T., and MacKinnon, R. (2002) *Nature* **415**, 287–294
23. Dutzler, R., Campbell, E. B., and MacKinnon, R. (2003) *Science* **300**, 108–112
24. Gründer, S., Thiemann, A., Pusch, M., and Jentsch, T. J. (1992) *Nature* **360**, 759–762
25. Ludewig, U., Pusch, M., and Jentsch, T. J. (1996) *Nature* **383**, 340–343
26. Friedrich, T., Breiderhoff, T., and Jentsch, T. J. (1999) *J. Biol. Chem.* **274**, 896–902
27. Accardi, A., Walden, M., Nguitrageol, W., Jayaram, H., Williams, C., and Miller, C. (2005) *J. Gen. Physiol.* **126**, 563–570
28. Li, X., Wang, T., Zhao, Z., and Weinman, S. A. (2002) *Am. J. Physiol.* **282**, C1483–C1491
29. Zuñiga, L., Niemeyer, M. I., Varela, D., Catalán, M., Cid, L. P., and Sepúlveda, F. V. (2004) *J. Physiol. (Lond.)* **555**, 671–682
30. Middleton, R. E., Pheasant, D. J., and Miller, C. (1996) *Nature* **383**, 337–340
31. Weinreich, F., and Jentsch, T. J. (2001) *J. Biol. Chem.* **276**, 2347–2353
32. Gaxiola, R. A., Yuan, D. S., Klausner, R. D., and Fink, G. R. (1998) *Proc. Natl. Acad. Sci. U. S. A.* **95**, 4046–4050
33. Greene, J. R., Brown, N. H., DiDomenico, B. J., Kaplan, J., and Eide, D. J. (1993) *Mol. Gen. Genet.* **241**, 542–553
34. Steinmeyer, K., Schwappach, B., Bens, M., Vandewalle, A., and Jentsch, T. J. (1995) *J. Biol. Chem.* **270**, 31172–31177
35. Jentsch, T. J., Steinmeyer, K., and Schwarz, G. (1990) *Nature* **348**, 510–514
36. Lorenz, C., Pusch, M., and Jentsch, T. J. (1996) *Proc. Natl. Acad. Sci. U. S. A.* **93**, 13362–13366
37. Geelen, D., Lurin, C., Bouchez, D., Frachisse, J. M., Lelièvre, F., Courtial, B., Barbier-Brygoo, H., and Maurel, C. (2000) *Plant J.* **21**, 259–267
38. Zifarelli, G., and Pusch, M. (2009) *EMBO J.* **28**, 175–182
39. Pusch, M., Ludewig, U., Rehfeldt, A., and Jentsch, T. J. (1995) *Nature* **373**, 527–531
40. Lurin, C., Geelen, D., Barbier-Brygoo, H., Guern, J., and Maurel, C. (1996) *Plant Cell* **8**, 701–711
41. Estévez, R., Boettger, T., Stein, V., Birkenhäger, R., Otto, M., Hildebrandt, F., and Jentsch, T. J. (2001) *Nature* **414**, 558–561
42. Lim, H. H., and Miller, C. (2009) *J. Gen. Physiol.* **133**, 131–138
43. Zifarelli, G., Soliani, P., and Pusch, M. (2007) *Biophys. J.* **94**, 53–62
44. Accardi, A., Lobet, S., Williams, C., Miller, C., and Dutzler, R. (2006) *J. Mol. Biol.* **362**, 691–699
45. Miller, C., and Nguitrageol, W. (2009) *Philos. Trans. R. Soc. Lond. B Biol. Sci.* **364**, 175–180